論文 Concept of Concrete Compressive Fracture Energy in RC Deep Beams without Transverse Reinforcement

Torsak LERTSRISAKULRAT[*1], Akinori YANAGAWA[*2], Maki MATSUO[*1] and Junichiro NIWA[*3]

ABSTRACT: A bending test program on the series of RC deep beams without transverse reinforcement with the effective depth, d, of 200, 400 and 600 mm has been performed. The beams are subjected to the concentrated load at the mid span. The distribution of the local strains inside specimens, both of concrete and reinforcements, has been measured. The test results confirm the localized compressive failure of concrete in the deep beams. Subsequently, the actual localized failure volume, V_p, and the fracture energy, G_{Fc}, of concrete which locally failed in compression of each beam specimen have been evaluated.

KEYWORDS: RC deep beam, localization in compression, fracture energy of concrete in compression, beam without transverse reinforcement

1. INTRODUCTION

The behavior of reinforced concrete beams at failure in shear is distinctly different from their behavior in flexure as the failure occurred abruptly without sufficiently advanced warning [1]. Furthermore, the diagonal cracks that develop are considerably wider than the flexural cracks, especially, for deep beams in which shear is being the significant parameter. Deep beams are structural elements having a shear span to effective depth ratio, *a/d*, not exceeding 1. Due to the geometry of deep beams, they behave as two-dimensional rather than one-dimensional members and are subjected to a two-dimensional state of stress. As a result, plane sections before bending do not necessarily remain plane after bending. The resulting strain distribution can be no longer considered as linear, and shear deformations that are neglected in normal beams become significant compared to pure flexure. Consequently, the stress distribution acting on the cross-section of the beam becomes nonlinear even at the elastic stage. At the ultimate limit state, the compressive stress distribution in the concrete would no longer be the same parabolic shape as in the normal beam.

At the final failure state of deep beams, the upper portion of the beams in the vicinity area under the location in which the load is applied, the crushing of concrete due to compression is usually observed together with the compressive failure along the compressive arch directions (diagonal cracks) which connecting the loading point and supports. Owing to the fact that, the failure of concrete in compression is localized [2], [3], the descending path of the stress-strain curve is size-dependent and cannot be considered as material property. For this reason, in the analysis of reinforced concrete beams, more accurate results can be expected if the effects of localization in compression are taken into account.

Therefore, in this paper, an experimental program on a series of deep beams without transverse reinforcement subjected to the concentrated load at the mid span has been conducted in order to observe the actual compressive shear failure behavior. Besides, by utilizing the techniques of local

*1 Department of Civil Engineering, Tokyo Institute of Technology, Member of JCI
*2 Department of Civil Engineering, Tokyo Institute of Technology
*3 Department of Civil Engineering, Tokyo Institute of Technology, Prof. Dr., Member of JCI

strain measurement [4], the observation on the localized compressive failure of the RC deep beams has been carried out. Finally, the localized compressive failure volume has been evaluated and the fracture energy of the concrete which failed in compression in the deep beams has been calculated.

2. EXPERIMETAL INVESTIGATIONS

2.1 OUTLINES OF THE TESTS

Deep beams with the effective depth, d, of 200, 400 and 600 mm with the loading span of 0.40, 0.80 and 1.20 m (overall length is equal to loading span plus 0.60 m), respectively, were cast and reinforced with deformed PC bars as tensile reinforcement. All beams were 150-mm wide and the concrete cover from the center of the PC bars to the tensile face of all beams was 50 mm. The details of the dimension and reinforcements of the specimens are shown in **Table 1** together with the schematic diagram of the specimen as depicted in **Fig. 1**.

In order to measure the local strains inside the beams, the deformed acrylic bars attached by strain gages with the interval of 30 mm were embedded inside each specimen as shown in **Fig. 2 (a)** to **(c)**. In addition to the acrylic bars, the strain gages were also attached to both the top and bottom reinforcements. **Fig. 3 (a) to (c)** shows the photos of the beam before casting and the strain gages attached to the reinforcements. It is noted that the anchor plates and bolts were employed at both ends of the beam in order to ensure the sufficient anchorage between concrete and deformed PC bars (**Fig. 4**).

Table 1 Outlines of the experiments

Designation	d, mm	h, mm	2a, mm	L, mm	r, mm	Deformed PC bars	Top Bars (SR235)	Vertical Steel (SD295A)
D200	200	250	400	460	50	PC-ϕ 19	ϕ 6	D6
D400	400	450	800	860	100	PC-ϕ 25	ϕ 6	D6
D600	600	650	1,200	1,260	150	PC-ϕ 32	ϕ 6	D6

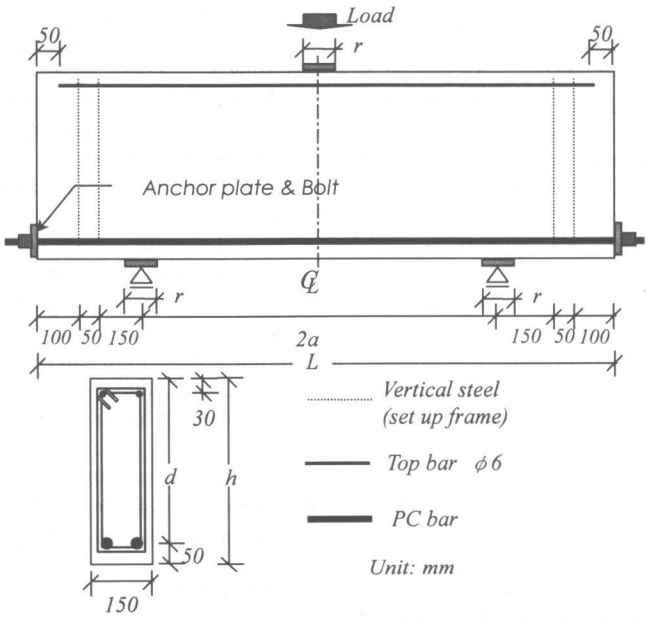

Fig. 1 Schematic drawing of specimen

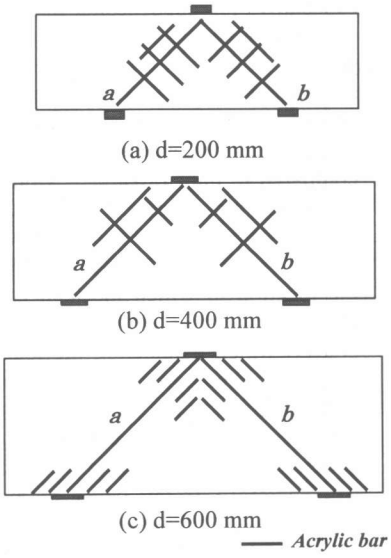

* *All strain gages were aligned parallel to the directions of the compressive arch on each side (direction of acrylic a and b).*

Fig. 2 Arrangement of acrylic bars

Table 2 Mixing proportion of concrete and mechanical properties of reinforcements

(a) Mixing proportion

W/C (%)	s/a (%)	Unit content (kg/m^3)			
		W	C	S	G
50	49	190	380	853	898

C: high early strength portland cement; S: river sand; G: crushed stone, max. size=13 mm; age of test 7 days, air content 2.5%; no water reducing agent or superplasticizer was used.

(b) Mechanical properties of reinforcements

Property	Size/Grade	Area, mm^2	E_s, N/mm^2	f_y, N/mm^2	f_u, N/mm^2
Top Bar	R6/SR235	28.27	-	310	452
Vertical Steel	D6/SD295A	31.67	-	331	509
Deformed PC Bar (Type B)	PC-ϕ19	286.50	2.01×10^5	1026	1127
	PC-ϕ25	506.70	2.00×10^5	1004	1130
	PC-ϕ32	794.20	2.01×10^5	1006	1147

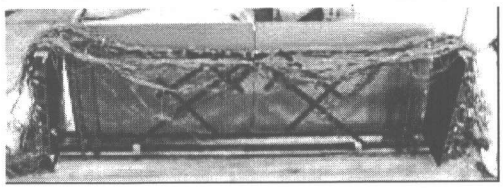

(a) Specimen before casting

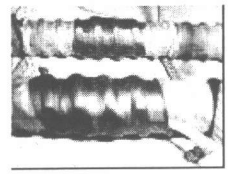

(b) PC bars

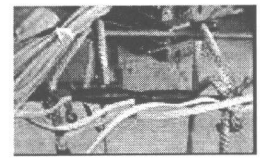

(c) Top bars

Fig. 3 Preparation of specimen before casting

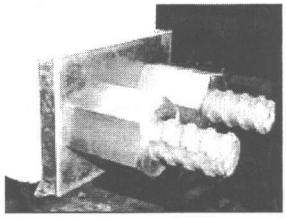

Fig. 4 End fixing of PC bars

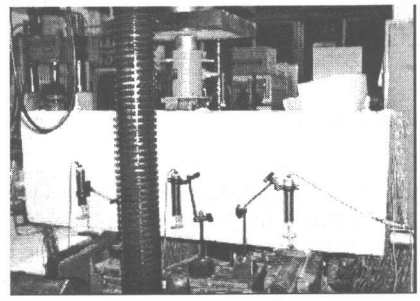

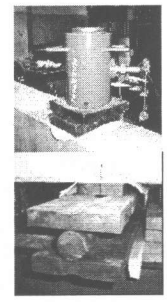

(a) Specimen set up before testing **(b)** Load cell and support

Fig. 5 Test set up

The concrete mixed with the maximum aggregate size 13 mm was used in casting of the beams. The mixing proportion of concrete and the mechanical properties of the reinforcements are summarized in **Table 2(a)** and **(b)**. All beams were subjected to the concentrated load at the mid span through the loading plate width, *r*, as shown in **Table 1** (r/d=0.25). At each support, a set of teflon sheets inserted by silicon grease was put over the steel plate (which has the same width as loading plate, r), in order to reduce the friction at the interface between the specimen and the supports and to ensure the lateral movement during the test. The deflection of the beam was measured by using deflection gages measured at both faces of the mid span and over the both supports. The horizontal movement of the beams has also been checked by a deflection gages installed horizontally at either end of a specimen. The test set up and the measurement were illustrated as shown in **Fig. 5**. During all tests, after the peak load was reached, the technique of one-directional repeated loading was utilized in order to capture the complete load-deflection curve.

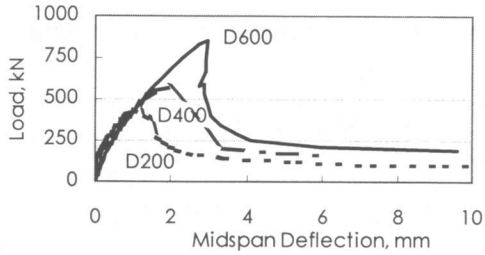

(a) Test results

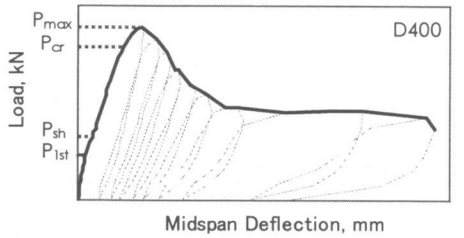

(b) Typical load-deflection curve (D400)

Fig. 6 Load-mid span deflection

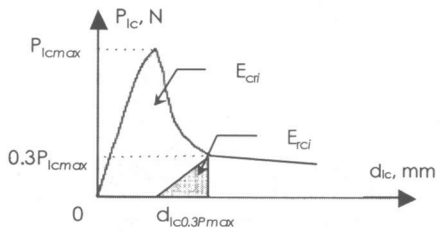

Fig. 7 Calculation of E_{cri}

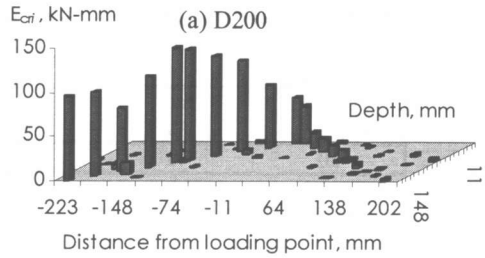

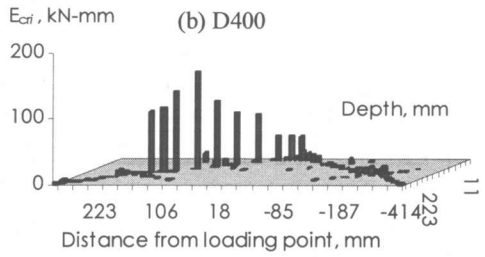

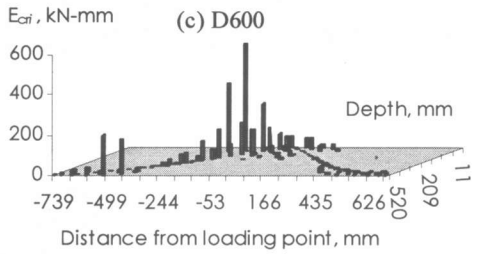

Fig. 8 Distribution of E_{cri}

2.2 EXPERIMENTAL RESULTS

From the test results, the external load-mid span deflection curve of the beams can be plotted as shown in **Fig. 6(a)**, whereas **Fig. 6(b)** shows the typical load-mid span deflection curve. The test results are also tabulated in **Table 3**. On the other hand, the local load-displacement relationship of concrete along the compressive arch can be plotted. The local displacement, d_{lc}, is obtained by multiplying the measured local strain by the interval between strain gages, i.e. 30 mm, whereas, the local load, P_{lc}, is the evaluated load applying to the diagonal strut, which is equal to external load divided by 2sin45°. Subsequently, the energy consumed locally by concrete, E_{cri}, can be calculated from the area under the local load-displacement curve of each gage, up to the load level of 30 percent of maximum load, excluding the recoverable portion, E_{rci} (**Fig. 7**). The distribution of E_{cri} plotted in **Fig. 8(a)** to **(c)** shows that only some portions of concrete absorbed most of the energy while some portions absorbed very small or almost zero amount of energy. That means, when a deep beam failed in compressive shear, the localization in compression occurred along the compressive arch direction, which connecting the point of load application and supports, and in vicinity of the loading point.

In the test, the compressive shear failure mode and adequate concrete covering of the beam were enhanced by employing the high strength deformed PC bars. In addition, according to the results from the strain gages attached to the PC bars and top bars at the mid span, it was found that the maximum stress of the bars are far below the yielding limit in all cases. In addition, because of the small cross-section size (10 × 10 mm) and low modulus of elasticity, compared with that of concrete and reinforcements, of the deformed acrylic bars, the shear resistance caused by the bars embedded perpendicular to acrylic bars a and b will be neglected.

Table 3 Summation of test results

Specimen	P_{1st}, kN	P_{sh}, kN	P_{cr}, kN	P_{max}, kN	f_c', N/mm^2	f_t, N/mm^2	G_F^*, N/mm	V_p, $\times 10^6$ mm^3	E_{ext}, kN-mm	G_{Fc}, N/mm^2	$G_{Fc}'^{**}$, N/mm^2
D200	125.6	157.0	304.1	428.3	38.4	3.4	0.16	4.05	891	0.220	0.214
D400	127.5	181.5	515.0	570.6	35.5	3.0	0.16	5.94	1,420	0.239	0.210
D600	215.8	245.3	588.6	848.9	40.8	2.4	0.16	10.08	2,165	0.215	0.217

** G_F is the fracture energy of concrete in tension.*

*** G_{Fc}' is the compressive fracture energy of concrete from the uniaxial compressive test.*

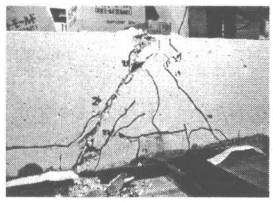

(a) D200

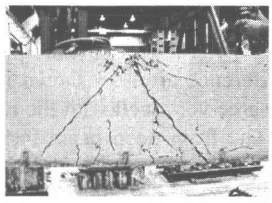

(b) D400

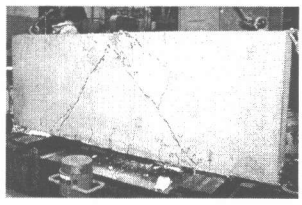

(c) D600

Fig. 9 Failure of specimens

2.3 CRACKING AND FAILURE OF DEEP BEAMS

Cracking started with the development of a few fine vertical flexural cracks at the mid span, at the first cracking load, P_{1st}. Then, few inclined shear cracks suddenly developed and proceeded to propagate toward the neutral axis from the supports to the portion in which the external load was applied as it can be seen from the swiftly change of the slope of the load-deformation curve when the shear cracking load, P_{sh}, was reached (**Fig. 6 (b)**). It is noted that the directions of the observed diagonal cracks are corresponding to the directions of the embedded acrylic bars a and b.

When the beam was further loaded, the crushing of concrete in the vicinity of loading point started at the crushing load, P_{cr}. Finally, the beam reached the maximum resistance at the peak load, P_{max}, and the failure took place as the principal inclined crack dynamically joined the crushed concrete zone. Anyway, it was observed that the severe failure took place only at one side of the beam. This is because of the fact that a reinforced concrete beam is not homogeneous and the strength of the concrete throughout the span is subjected to a normally distributed variation, hence the stabilized failure diagonal crack at both ends of the beam cannot be expected as can be seen from the photos shown in **Fig. 9 (a)** to **(c)**.

3. COMPRESSIVE LOCALIZED FAILURE VOLUME, V_p, AND COMPRESSIVE FRACTURE ENERGY OF CONCRETE, G_{Fc}

By considering the shape of concrete local load-displacement curves, which showed the softening and unloading behavior, together with the comparison with the length of severe diagonal compressive failure zone along the direction of compressive arch observed during the experiment, the criterion for determining the localized compressive failure zone has been introduced. It was found that the zone in which the E_{cri} is larger than 1 percent of the summation of E_{cri} of all gages along the directions of compressive arch (acrylic bars a and b, **Fig. 2**), E_{cr}, can be judged as the failure zone and the length of the zone, so-called localized compressive failure zone, L_p, can be evaluated. The width of the localized compressive failure zone, w_p, is estimated to be equal to twice the distance between the 2 adjacent acrylic bars parallel with the directions of acrylic bars a and b, i.e. 100 mm for D200 and 150 mm for D400 and D600. Finally, when the failure assumed to occur throughout the width of the beam, b, the localized compressive failure volume, V_p, is the product of L_p times w_p and b, as shown in Eq. 1. The results of V_p are summarized in **Table 3**.

$$V_p = L_p \times w_p \times b \tag{1}$$

Because the compressive fracture energy of concrete, G_{Fc}, is defined as the energy required to cause compressive failure to a unit volume of concrete, therefore, G_{Fc} is computed based on the

obtained V_p and the externally applied energy that caused unrecoverable failure to concrete, E_{ext}. Likewise the concept in calculating E_{cri}, E_{ext} is calculated from the area under the external load-mid span deflection curve excluding the part that can be recovered when unloaded, E_{rc}. It should be noted that, as mentioned above, the reinforcements were not yielded in all cases, hence the deduction of E_{ext} due to the permanent deformation of reinforcements are not required. Then, G_{Fc} is obtained by dividing the E_{ext} by V_p, as shown in Eq. 2 and the results have been summarized in **Table 3**. The calculation of energy was done up to about 30 percent of P_{max} of the descending path of curve in which the gradient of curves became flat.

$$G_{Fc} = E_{ext} / V_p \qquad (N/mm^2) \qquad (2)$$

Furthermore, according to authors' previous research [3], it has been found that the relationship between the concrete cylindrical compressive strength, f_c', and the concrete compressive fracture energy when subjected to uniaxial compressive load, G_{Fc}', can be shown by the following Eq. 3.

$$G_{Fc}' = 0.86 \times 10^{-1} f_c'^{1/4} \qquad (N/mm^2) \qquad (3)$$

Then, the comparison between G_{Fc}, obtained from the deep beam tests, and G_{Fc}', from the uniaxial compression tests, has been proceeded. The results are plotted as shown in **Fig. 10**. The percentages of difference are also shown in the parenthesis. It can be seen that the results from the deep beam tests agree very well with the results of the uniaxial compressive tests. However, it can be noticed that G_{Fc} from deep beam tests are higher than G_{Fc}' from the uniaxial compression tests in all cases. This is because the calculation of E_{ext} is including also the energy which causes the flexural cracks (at the bottom of the mid span) to the beams, nevertheless it is negligibly small compared with the energy consumed by the diagonal cracks. This shows that, if the compressive localized failure behavior of concrete has been incorporated into the analysis properly, the more accurate predictions on the behavior of deep beams will be obtained.

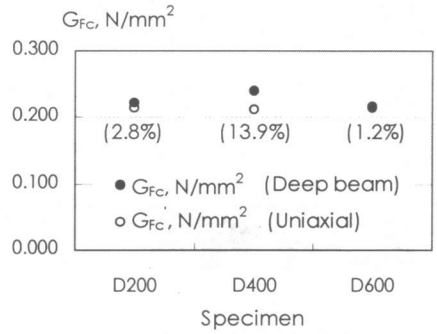

Fig. 10 Compressive fracture energy, G_{Fc}

4. CONCLUSIONS

From the experimental results, by measuring the strain distributions inside RC deep beams, the occurrence of concrete localized compressive failure in the deep beams has been confirmed. The compressive localized failure volume can be determined based on the measured local strain and relative energy consumed by concrete. Subsequently, the compressive fracture energy of concrete has been evaluated based on the obtained compressive localized failure volume and the externally applied energy that caused the compressive failure of concrete. Finally, the comparison between the obtained compressive fracture energy of concrete in the deep beams and that of the uniaxial compression has been conducted and shows good agreement.

REFERENCES

1. Edward, G.N., "Reinforce Concrete: a fundamental approach," Prentice hall, 1990, pp.145-154.
2. Santiago, S.D. and Hilsdorf, H.K., "Fracture Mechanisms of Concrete under Compressive Loads," Cement and Concrete Research, Vol.3, 1973, pp.363-388.
3. Torsak, L. et. al., "Experimental Study on Parameters in Localization of Concrete Subjected to Compression," Journal of Materials, Concrete Structures and Pavements,, JSCE, No.669, Vol.50, 2001, pp.309-321.
4. Nakamura, H. and Higai, T., "Compressive Fracture Energy and Fracture Zone Length of Concrete," JCI-C51E Seminar on Post-Peak Behavior of RC Structures Subjected to Seismic Loads, Vol.2, 1999, pp.259-272.